Self-localization from Images with Small Overlap

Tanaka Kanji

Abstract— With the recent success of visual features from deep convolutional neural networks (DCNN) in visual robot self-localization, it has become important and practical to address more general self-localization scenarios. In this paper, we address the scenario of self-localization from images with small overlap. We explicitly introduce a localization difficulty index as a decreasing function of view overlap between query and relevant database images and investigate performance versus difficulty for challenging cross-view self-localization tasks. We then reformulate the self-localization as a scalable bag-of-visual-features (BoVF) scene retrieval and present an efficient solution called PCA-NBNN, aiming to facilitate fast and yet discriminative correspondence between partially overlapping images. The proposed approach adopts recent findings in discriminativity preserving encoding of DCNN features using principal component analysis (PCA) and cross-domain scene matching using naive Bayes nearest neighbor distance metric (NBNN). We experimentally demonstrate that the proposed PCA-NBNN framework frequently achieves comparable results to previous DCNN features and that the BoVF model is significantly more efficient. We further address an important alternative scenario of "self-localization from images with NO overlap" and report the result.

I. INTRODUCTION

With the recent success of visual features from deep convolutional neural networks (DCNN) in visual robot self-localization, it has become important and practical to address more general self-localization scenarios. Self-localization aims to use a robot's visual image as a query input and to search over a database of pre-mapped images to locate a relevant database image that is viewed from the nearest neighbor viewpoint to the query image's viewpoint. Recently, it has been found that the intermediate responses of a DCNN can be viewed as a discriminative feature for image matching. In [1], the DCNN descriptor is exploited for the image retrieval task where DCNN descriptors are translated to short vectors by PCA dimension reduction. In [2], DCNN descriptors are applied to visual robot self-localization tasks and produce impressive results.

In this paper, we address the problem of self-localization from images with small view overlap. This is a challenging scenario with important applications including self-localization using far features [3], object co-segmentation [4], sparse feature maps [5], and the lost robot problem [6]. To date, the majority of the existing work on self-localization, including those with DCNN features, rely on
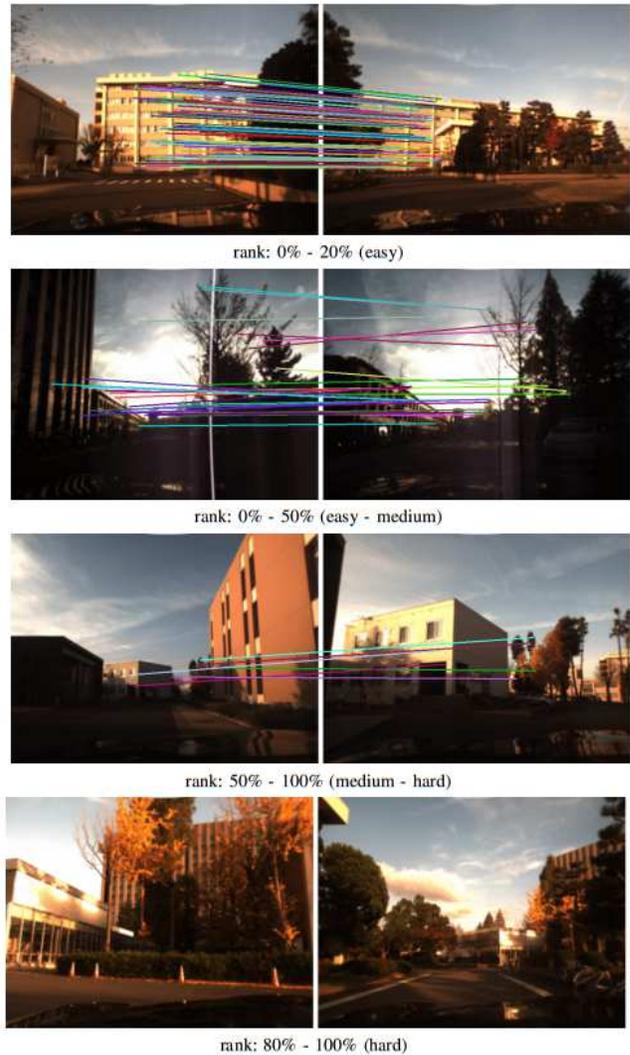
Fig. 1. Self-localization with different levels of localization difficulty index (LDI). The LDI of a self-localization task is a decreasing function of view overlap between the query and relevant database image pair. In experiments, we employ SIFT matching with VFC verification (colored line segments) to evaluate the amount of view overlap. All the pairs in the dataset are evaluated and sorted according in ascending order of LDI. Rank in the sorted list (normalized by the list's length) [%] can be viewed as a prediction of relative difficulty of the corresponding self-localization task. Displayed in figures are samples from self-localization tasks with four different levels of ranks [%].

a strong assumption: there is a large view overlap (e.g., $> 50\%$) between the query and relevant database images. In general cases where the overlap between two relevant views is frequently small (e.g., $\leq 10\%$), the self-localization

problem is largely unsolved.

To address the above issue, we explicitly introduce a localization difficulty index as a decreasing function of view overlap between the query and relevant database images (Fig. 1), and investigate the performance versus difficulty of challenging cross-view self-localization tasks. We collected a dataset of view images with ground truth viewpoints, and evaluated amount of view overlap for each relevant image pair by employing techniques of common visual pattern discovery [7]. We experimentally determined that DCNN features fail in the case of small overlap owing to a large number of outlier features and occlusions. We further address the challenging and important scenario of "self-localization from images with NO overlap" and report the result.

We then reformulate the self-localization as a scalable bag-of-visual-features (BoVF) scene retrieval [8] and present an efficient solution called PCA-NBNN, aiming to facilitate fast, yet discriminative correspondence between partially overlapping images. The basic idea is to encode local part-level DCNN features of a scene image into a BoVF document model and then apply an effective document retrieval technique for efficient indexing and search. Our encoding model adopts recent findings in discriminativity preserving encoding of DCNN features [1] where principal component analysis (PCA) compression provides efficient short codes that provide state-of-the-art accuracy on a number of recognition tasks. We also adopt a naive Bayes nearest neighbor distance metric (NBNN), inspired by our previous IROS15 paper, that has proven to be effective in an alternative application of cross-domain scene matching based on SIFT features [9]. In experiments, we confirm that the proposed framework frequently achieves comparable results to previous DCNN features even though the BoVF model is significantly more efficient.

A. Relation to Other Work

The main contribution of this paper is in investigating the use of DCNN features in challenging cross-view self-localization scenarios and presenting an efficient recognition approach based on a BoVF scene model. The BoVF subsystem employed in III-A is inspired by a bag-of-parts model in the authors' previous ICRA15 paper [10].

Scene descriptors for visual place recognition (VPR) problems have been studied extensively. Local feature approaches such as BoVF scene descriptors have been widely studied from various aspects [11] including confusing features, quantization errors, query expansion, database augmentation, vocabulary tree, and global spatial geometric verification as post-processing. As suggested by previous studies [12] and also by our ICRA15 paper [13], existing BoVF models are not sufficiently discriminative and frequently fail to capture the appearance changes across domains.

Global feature approaches such as the GIST feature descriptor [14] (where a scene is represented by a single global feature vector) are compact and have high matching speeds. In the robot vision community, global feature approaches have been widely used in the context of cross-domain VPR

Fig. 2. Experimental environments. Red, yellow, and green lines: viewpoint paths on which dataset #1, #2, and #3 were collected.

[12], [15], [16]. [12] introduces a robust VPR framework called SeqSLAM for cross-season navigation tasks separated by months or years and opposite seasons. More recently, in [2], the authors demonstrated that DCNN features outperform the majority of the existing global features in typical VPR tasks.

In this study, the proposed approach is built on some of our previous techniques including compact binary landmarks of deep network in ICRA10 [17], compact projection in IROS11 [18], NBNN scene descriptor in IROS15 [9], and bag-of-parts in ICRA15 [10]. However, the current study focuses on the use of DCNN features in visual robot localization.

DCNN features have received considerable attention in the past years. However, effective use of DCNN descriptors in the context of robot localization has not thus far been sufficiently explored and a main topic of on-going research [2]. In particular, the issue of view overlap as localization difficulty index and the use of the PCA-NBNN model to address partially overlapping views have not been addressed in existing studies.

II. PROBLEM

A. Dataset

For clarity of presentation, we first describe the experimental system by which a dataset is collected in our university campus (Fig. 2) and used as a benchmark for performance comparison in the experimental section. Although our application scenario is single-view self-localization, we employed a stereo SLAM system with visual odometry to collect a set of view images with ground-truth viewpoint information. Our stereo SLAM system is built on a Bumblebee stereo vision camera system and visual odometry [19] and follows the standard formulation of pose graph SLAM [20]. We used images with size 640×480 [pixels] from the left eye view of the stereo camera as the image dataset.

B. Localization Performance Index

We conduct a series of $N^E = 1,800$ self-localization tasks using a set of N^E independent subsets of the dataset. For each task, we sample one image I^Q as a query input, one image I^R as a relevant image, and a size $N^D - 1$ image collection ($N^D = 100$) as destructor images $\{I^D\}_{i=1}^{N^D-1}$ so that
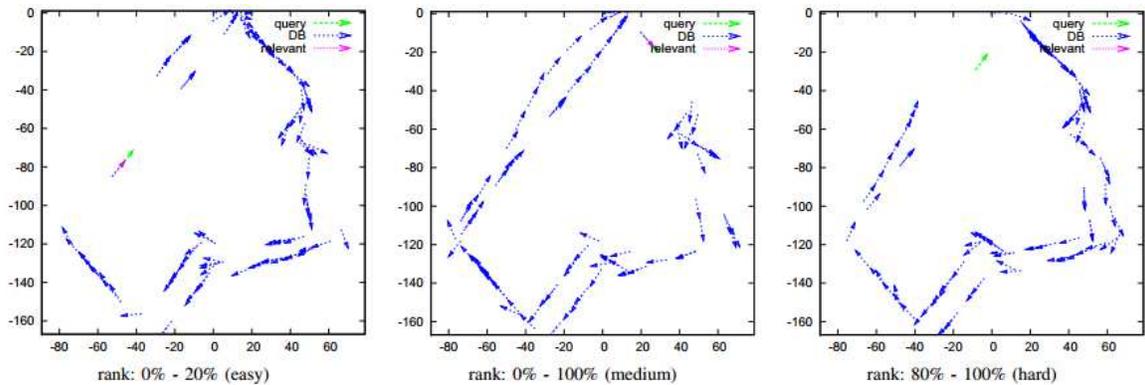
Fig. 3. Sample configurations of viewpoints for different levels of localization difficulties.

its viewing angle is different from the query image's viewing angle by T^θ or its viewing area $V(p^D)$ does not overlap with the query image's viewing area $V(p^Q)$, where p^D and p^Q are the ground-truth viewpoints of the destructor and the query images. In this case, the viewing area is empirically defined as an isosceles-triangular region with an apex angle of 40 deg and the length of a leg as 50 m.

Localization performance is measured by its recognition rate. Given a query image, its retrieval result is in the form of a ranked list of database images (with length N^D). Then, the recognition rate y is defined over a set of self-localization tasks, as the ratio y of tasks whose relevant database images are correctly included in the top x ($x \le N^D$) ranked images.

C. Localization Difficulty Index

The core of the localization difficulty index (LDI) is the evaluation of the view overlap between the relevant pair of query and database images. Intuitively, the amount of view overlap can be evaluated by counting the number of local features matched between the relevant pair. In this study, we tested three different strategies for local feature matching: SIFT matching without any post verification [21], SIFT matching with geometric verification by RANSAC [22], and using vector field consensus (VFC) [7]. We determined that VFC stably produces acceptable results. SIFT-matching frequently produces many false positives and is not effective to identify image pairs with small overlap. RANSAC geometric verification is effective only when there are many structured objects such as buildings and does perform well in general cases. Conversely, VFC is stable and able to produce many true matches; it performs well in both structured and unstructured scenes. Based on this result, we elected to implement VFC as the method for evaluating view overlap in the following experiments.

Localization difficulty index $D(I^{query})$ is now defined as a decreasing function of view overlap $O(\cdot, \cdot)$ between query image I^{query} and its relevant image $I^{relevant}$:

$$D(I^{query}) = 1 / \left[O(I^{query}, I^{relevant}) \right]. \quad (1)$$

Predicting localization difficulty from such an image based cue is an ill-posed problem; it is impossible to design a perfect prediction method. Rather, our strategy for difficulty

prediction is based on the *relative* LDI value. More formally, we sort all the N^E self-localization tasks in ascending order of LDI and then compare the difficulty of different self-localization tasks by using its rank within the sorted list normalized by the list's length [%]. To create a dataset, we sample pairs of query and its relevant database images from a range of normalized rank $[rank^{min}, rank^{max}]$, in which the parameters $rank^{min}$% - $rank^{max}$%, control the relative difficulty of the dataset. In practice, we observed that this prediction method performed effectively. Fig. 3 displays samples of viewpoints used in the experiment for three distinct cases corresponding to three different levels of LDI.

III. METHODS

The proposed PCA-NBNN approach consists of three distinct steps: (1) modeling, (2) encoding and (3) retrieval of scenes, each of which is detailed in the following subsections.

A. Modeling by Bag-of-Scene-Parts

Scene modeling is an important first step in visual robot self-localization. The objective of scene modeling is to convert a robot's view image to an invariant scene descriptor, which allows a robot to search over an environment map or a collection of pre-mapped view images to identify similar views. The main problem we faced was how to describe a scene discriminatively and compactly, both of which are necessary to manage the geometric/photometric view changes and the significant amount of visual information. The proposed approach is inspired by the fact that even DCNN features frequently fail to capture the local parts of a scene, as we will see in the experimental discussion, Section IV. Typically, it is weak against large view changes and frequently produces poor results in visual robot localization. Hence, we adopt a kind of bag-of-parts scene model [23], where each query/database image is described by an unordered collection of part-level features, to facilitate fast, yet discriminative correspondence between partially overlapping images.

A key design issue is how to discover useful parts in a scene. This is different from the problem of object segmentation, i.e., segmenting an image into meaningful parts
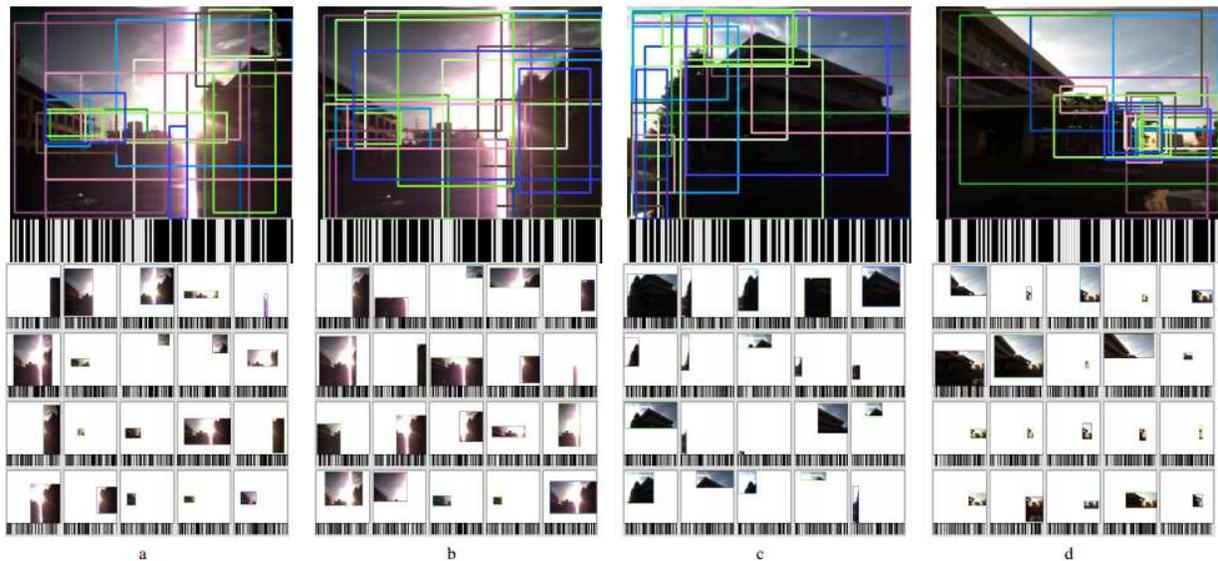
Fig. 4. Compact binary landmarks. a, b, c, and d: 4 different examples of a query image (top) being explained by one image-level feature and 20 part-level features (bottom). Each scene part is further encoded to a 128-bit binary code, which is visualized by a barcode.

such as objects, which is a core problem in the field of computer vision [24]. Rather, our goal is to realize consistent segmentation for similar view images, allowing a robot to obtain similar parts for similar scenes (i.e., relevant scene pair). In general, any part-segmentation technique such as clusters of superpixels described in our ICRA15 paper [10], can be adopted. In the current study, we borrow techniques from the unsupervised object detector [25], which quantifies how likely it is for an image window to contain an object of any class. We first extract the set of 100 bounding boxes with the highest objectness score and then rerank these according to the area of the bounding box and select the top $(N^P - 1)$ ranked parts. In total, we obtain a size $N^P = 21$ set of DCNN features consisting of one image-level feature and 20 part-level features.

B. Encoding by Experience-based Vocabulary

We then encode the scene parts to a bag-of-parts representation [23]. First, we extract a 4,096 dimensional DCNN feature from a region that corresponds to the bounding box of each scene part. Although a DCNN is composed of a number of layers, in each of which responses from the previous layer are convoluted and activated by a differentiable function, we use the sixth layer of DCNN, as it has proven to produce effective features with excellent descriptive power in previous studies [26]. Then, we perform PCA compression to obtain 128 dimensional features. Our strategy is supported by the recent findings in [1] where PCA compression provides excellent short codes with 512, 256, and 128 short vectors that provide state-of-the-art accuracy on a number of recognition tasks. In our experiments, we use DCNN features from the database to train the PCA models for different settings of the output dimension, 512, 256, and 128.

Another key design issue is an efficient scene retrieval. The

bag-of-parts representation, presented above, is a relatively compact and discriminative scene descriptor. However, it is a high dimensional description and does not directly realize high-speed scene retrieval. To address this issue, we adopt the nearest neighbor approach [9] where each local feature is explained by its nearest neighbor (NN) library features. Because the original local feature can be compactly represented by the IDs of NN library features, efficient data structures such as inverted files can realize compact indexing and fast retrieval.

One of the most popular instances of the NN approach is the bag-of-words (BoW) [8], a well-established technique for image retrieval. Its key component is offline dictionary learning. That is, offline, a set of visual features are extracted from training images and then a dictionary of exemplar visual features are learned by unsupervised learning algorithms such as k-means clustering. Once such a dictionary is learned, a given image is translated to an unordered collection of NN library features, each of which is compactly represented by the ID of the NN library feature, which is termed visual word. This pre-learning of the dictionary is effective to achieve fast retrieval. Conversely, a known limitation of the BoW model is its vector quantization effect, which significantly reduces the descriptive power of the BoW descriptor.

We address the above issue by an experience-based fine vocabulary. As a key difference from the BoW approach, we directly employ a library of available visual features, i.e., not the vector quantized version, termed visual experience. This strategy is motivated by the fact that an enormous amount of visual experience is readily available, such as a collection of visual images acquired in the robot's previous navigation or shared by colleague robots, as well as images crawled from the web. Because the proposed approach does not rely on vector quantized visual features, database features
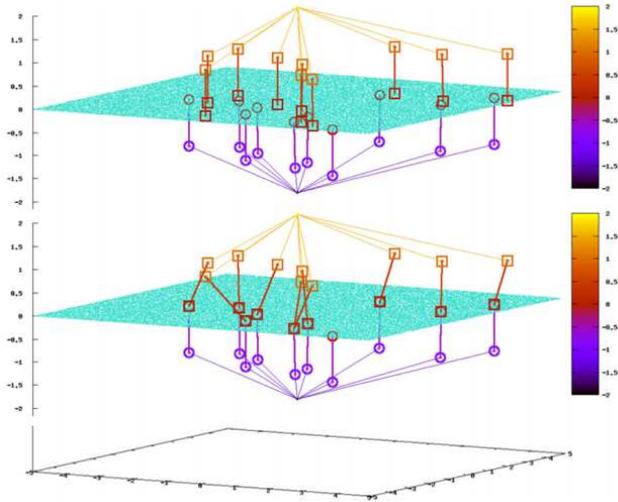
Fig. 5. Effect of asymmetric distance computation (ADC). The figures compare the two different encoding schemes, BoW (top) and ADC (bottom), using a toy example of a 2D feature space x-y, in the case of the fine library. In the figures, query/database images are located $z = 2/z = -2$, local features extracted from query/database images are located $z = 1/z = -1$, and library features (green dots) including NN library features (colored small boxes) are located $z = 0$. Previous BoW systems (top), which encode both query and database features, frequently fail to identify common library features between query and database images in the case of our fine library. Conversely, ADC, which encodes only database features, not query features, is stable to identify NN library features of individual database features by an online search over the space of library features (i.e., $z = 0$).

Fig. 6. Performance vs. difficulty. Vertical axis: ratio of self-localization tasks where the ground truth image pair is top-X ranked for ten different ranges of rank X (X: 0.0-0.1, 0.1-0.2, ... , 0.9-1.0.). Horizontal axis: view overlap in terms of number of VFC matches, which is a decreasing function of localization difficulty index.

are expected to be approximated by many more similar NN library features. For example, in [10], we explored an approach for common landmark discovery aiming at unsupervised discovery of part-level library features that effectively explain a given input image. In this study, we employ a simple nearest neighbor-based distance metric to identify a library feature that approximates a given database feature.

We define place class as a collection of NN library features that approximates a given database image. To evaluate the dissimilarity between a query and a place class (i.e., database image), we propose to employ the image-to-class distance. This strategy is inspired by our previous IROS15 paper [9], where image-to-class distance was successfully applied to an alternative scenario of cross-domain localization using SIFT features. Let I and C denote a given query image and a place class (i.e., database image), both are represented by a set of local features ($I = \{f\}$, $C = \{f'\}$), then image-to-class distance is defined by:

$$f(I,C) = \sum_{f \in I} \min_{f' \in C} |f - f'|_2^2. \qquad (2)$$

C. Retrieval by Asymmetric Distance Computation

The proposed scene retrieval strategy is an instance of asymmetric distance computation (ADC), which only encodes the local features of the database; not the query local feature (Fig 5). This is in contrast to symmetric distance computation (SDC) employed by typical BoW systems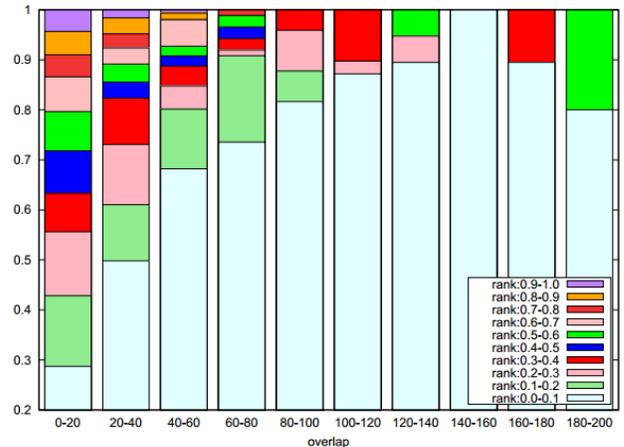, which encodes both query and database features. We have observed that the SDC strategy performed poorly in the case of our enormous and unorganized visual experience-based library owing to near duplicate and useless library features. In fact, there is virtually no probability that a query image and its relevant database image have the same NN library features in common (Fig. 5 top). Hence, we encode only database features and we directly match a query feature and each database image's NN library features (Fig. 5 bottom).

ADC is more accurate than SDC and employed in some previous systems in different contexts [27]. In our view, ADC functions even when there are many near duplicate library features, which is the case of our fine library. As another advantage, ADC allows an incremental update (e.g., deletion/insertion of features) of the database and the library, which is an important property from the viewpoint of incremental mapping and localization [20].

However, ADC is computationally more demanding as it requires many-to-many comparisons between the query and database images. To address this issue, we employ a compact binary encoding of images and fast bit-count operation that enables fast image comparison (Fig. 4). Query and library features are encoded to N_1 bit binary codes using the compact projection technique borrowed from [26] and [18] and compared by Hamming distance. Another limitation of the original NBNN distance metric is that it must pre-define a set of place classes. To address this, as mentioned, our algorithm mines the available visual experience (i.e., library) to locate similar N^p NN library features that effectively explain the database feature, in the same spirit as in our previous IROS14 paper [28], and then use the set of mined N^p library features as the place class that corresponds to the database image. Then, we compute the image-to-class distance between the query image to each place class by (2).

IV. EXPERIMENTS

We evaluated the performance over three independent datasets that were collected from different routes and view-
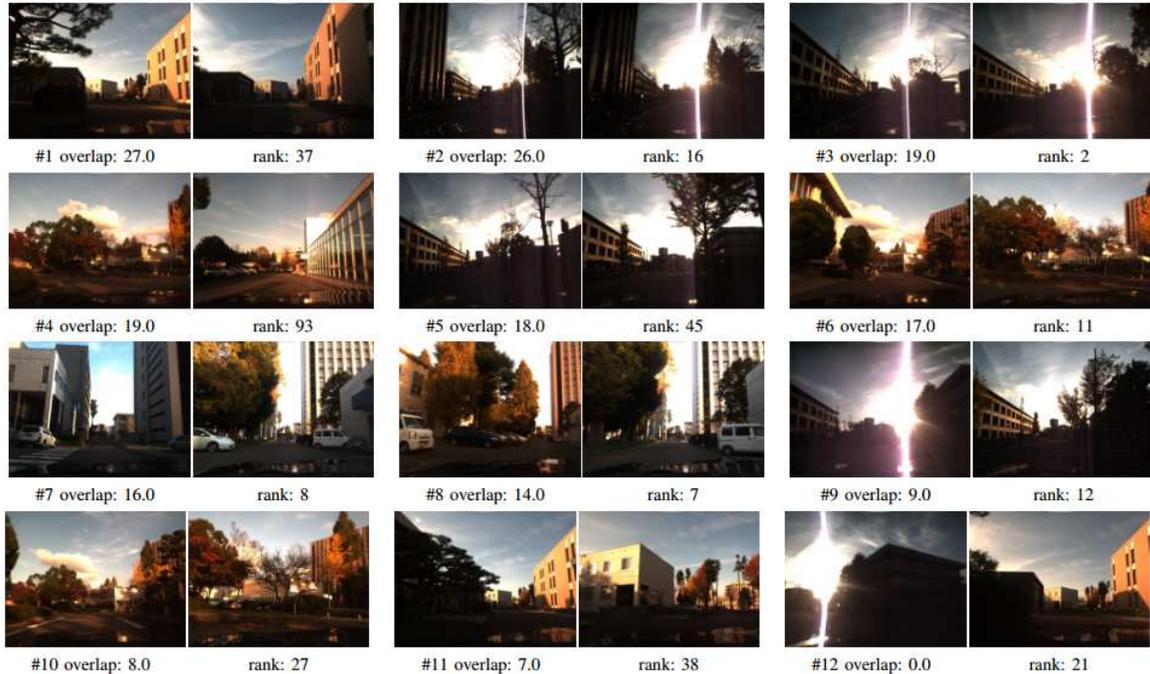
Fig. 7. Samples of self-localization tasks. Displayed in figures are samples of self-localization tasks (using "bodw20" algorithm). We uniformly sampled them from the experiments. For each sample, its query image (left) and the relevant database image (right) are displayed with the view overlap score ("overlap") as well as the localization performance ("rank"). Here, "rank" is the rank assigned to the ground-truth database relevant image, within a ranked list output by the recognition algorithm. From top to bottom, left to right, these samples are displayed in descending order of view overlap (i.e., from easiest to hardest).

points. The datasets used in these experiments consisted of collections of view images captured around a university campus, using the vision system described in II-A. Fig. 2 presents an overhead view of our experimental environment and viewpoint paths. For each viewpoint path, we acquired a collection of dense view images. Occlusion is severe in all the scenes and people and vehicles are dynamic entities occupying the scenes. Moreover, viewpoints are close to each other, which produces many near-duplicate database images and makes self-localization more difficult.

We investigated self-localization performance versus difficulty, based on the performance difficulty index introduced in II-C. First, a number of samples of sets of query, relevant database image, and destructor database images were generated, and sorted according in ascending order of the LDI defined in (1). Then, five different sets of 100 self-localization tasks with different levels of difficulty for each of the three viewpoint paths were sampled from rank 0%-20%, 0%-50%, 0%-100%, 50%-100%, and 80%-100% of the sorted list of self-localization tasks. Note that our strategy of down-sampling the original image set to a small (i.e., size 100) subset does not sacrifice self-localization difficulty as long as we use the recognition rate (defined in II-B) as the performance index.

In the experiments, different versions of image-level and part-level DCNN features were compared. Image-level DCNN features include the original 4,096-dim DCNN descriptor ("dcnn"), its PCA compressed 128-dim, 256-dim and 512-dim descriptors ("pca128", "pca256", and "pca512"),

and "pca128" descriptor is further compressed by compact projection to 20-bit, 16-bit and 12-bit code ("bin20", "bin16", and "bin12"). For the sake of reproducibility, we simply use the full libraries with size 2^{20}, 2^{16} and 2^{12} respectively for the 20-bit, 16-bit and 12-bit codes. Part-level DCNN features ("bodw20", "bodw16", and "bodw12") are different from "bin20", "bin16", "bin12" only in that they are originated from not only the image-level DCNN feature but also from part-level DCNN features, as described in III-A. Further, we also implemented an alternative part-level feature, termed "bodf", which is only different from the above "bodw20/16/12" in that the 128-dim PCA compressed part-level DCNN feature was used without binarization. We use the "bodf" only for the purpose of investigating the quantization loss caused by our compact projection. Note that in practice, the "bodf" method is not efficient and requires relatively high space and time cost.

Fig. 6 is a summary of distributions of self-localization performance versus view overlap, where the self-localization performance is measured in terms of the normalized rank of the relevant database image and the view overlap is measured by VFC matches.

Fig. 7 shows samples of query and database image pairs with view overlap score measured by VFC, together with performance results from 12 different self-localization tasks using the proposed "bodw20" method. The case #4 has relatively high "overlap" value due to false positive matches in the VFC verification, despite the fact that it is one of hardest self-localization tasks and in fact its self-localization
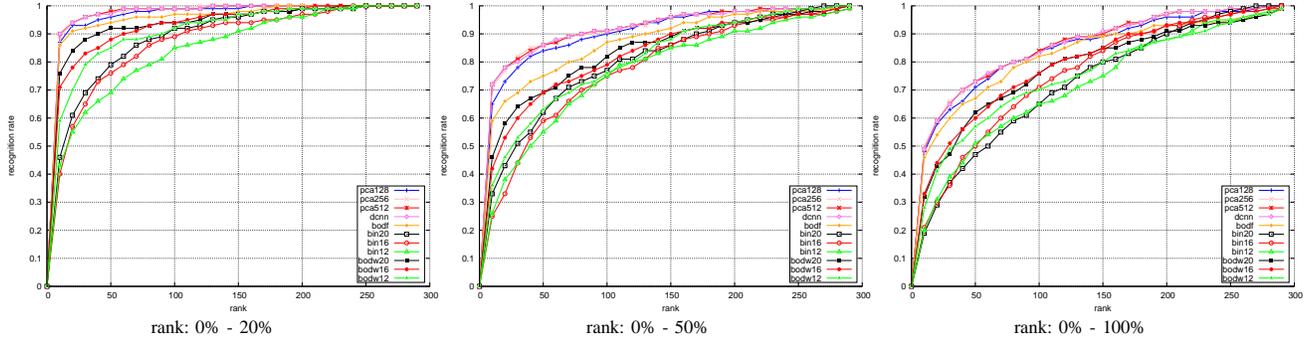
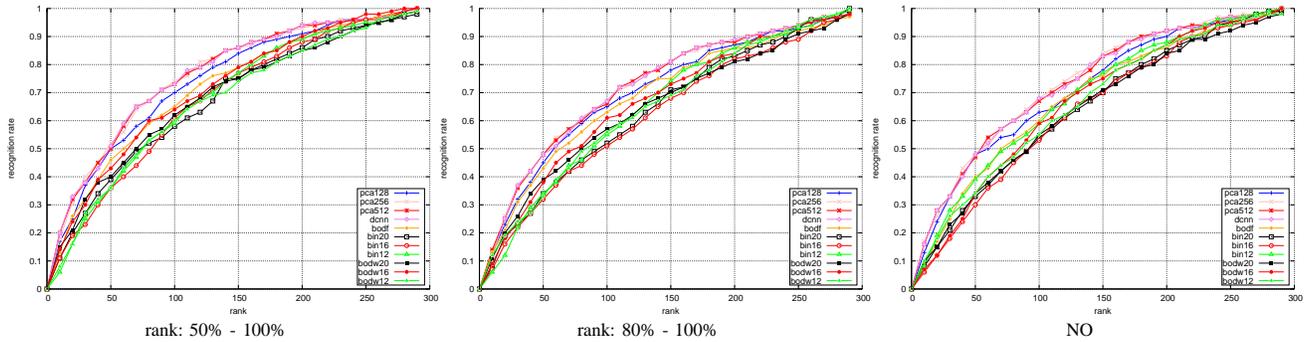Fig. 8. Localization performance on relatively easy localization scenarios.

Fig. 9. Localization performance on relatively hard localization scenarios.

performance is bad, rank = 93 %. The case #12 has 0 "overlap" value and despite the fact, recognition algorithm performs relatively well, rank = 21 %. For several cases, such as #1 and #5, occlusion is a major source of errors in place recognition. Despite the difficulty, it can be said that the proposed recognition algorithm stably performs well as will be shown in performance results (Figs. 8, 9).

Fig. 8 presents the results for relatively easy self-localization tasks. Note that for the "rank: 0% - 20%" dataset, the proposed method "bodw20" with fine ($2^{20}=$) 1M vocabulary performs relatively well despite the fact it is much more efficient than non-binarized DCNN features. Its rank-10% identification rate is approximately 0.9 and comparable to that of non-binarized DCNN features "dcnn" and high dimensional features "pca256" and "pca512". Unfortunately, the performance of the proposed method becomes relatively less than the non-binarized high-dimensional DCNN features for self-localization with medium level difficulty, as indicated in "rank: 0% - 50%" and "rank: 0% - 100%". This indicates relative robustness of non-binarized DCNN feature in self-localization with a medium level of difficulty.

Fig. 9 presents the results for relatively hard self-localization tasks. It can be seen that the proposed method "bodw20" again produces comparable results to 4,096-dim DCNN features. Its top-10% identification rate is comparable to that of non-compressed or PCA-compressed versions of DCNN features "dcnn", "pca128", "pca256", "pca512", and "bodf". This is because the fact that in the relatively hard self-localization scenarios, the performance of DCNN features drop drastically, because the query scene appears quite different from the relevant database scene. It can be said

that the proposed "bodw" method achieved good tradeoff between efficiency and descriptive power in the challenging scenario of self-localization from images with small overlap.

Finally, we investigated the case of "self-localization from images with NO overlap". More formally, we considered a hardest setting where the relevant database image with nearest neighbor viewpoint had zero overlap in terms of the number of matches by VFC. Fig. 9"NO" displays the results. It can be seen that DCNN features are better than chance (i.e., $y = x/300$). There are two reasons for this: (1) VFC may fail to detect matches even when there is view overlap between the relevant image pair; (2) views of relevant image pairs are frequently similar to one another owing to the atmosphere effect even when there is no view overlap. Overall, the proposed method "bodw20" is comparable to the non-binarized DCNN features, despite the fact that it is computationally significantly more efficient.

V. CONCLUSIONS

In this paper, we addressed the problem of self-localization from images with small overlap. We explicitly introduced a localization difficulty index as a decreasing function of view overlap between query and relevant database images and investigated performance versus difficulty for challenging cross-view self-localization tasks. We then presented a novel approach to bag-of-visual-features scene retrieval called PCA-NBNN to facilitate fast, yet discriminative correspondence between partially overlapping images. In experiments, we investigated localization performance versus difficulty and confirmed that the proposed method frequently yielded comparable performance with non-binarized high-

dimensional DCNN features. We further addressed an alternative important scenario of "self-localization from images with NO overlap", where the highly compressed PCA-NBNN feature is comparable to the previous high-dimensional DCNN features.

REFERENCES

[1] A. Babenko, A. Slesarev, A. Chigorin, and V. S. Lempitsky, "Neural codes for image retrieval," in *ECCV*, 2014, pp. 584–599.

[2] N. Sünderhauf, S. Shirazi, F. Dayoub, B. Upcroft, and M. Milford, "On the performance of convnet features for place recognition," in *IEEE/RSJ IROS*, 2015, pp. 4297–4304.

[3] C. Cadena, J. McDonald, J. Leonard, and J. Neira, "Place recognition using near and far visual information," in *Proc. the 18th IFAC World Congress*, 2011.

[4] H. O. Song, R. Girshick, S. Jegelka, J. Mairal, Z. Harchaoui, and T. Darrell, "On learning to localize objects with minimal supervision," *arXiv preprint arXiv:1403.1024*, 2014.

[5] L. Contreras and W. Mayol-Cuevas, "Trajectory-driven point cloud compression techniques for visual slam," in *IEEE/RSJ IROS*, 2015, pp. 133–140.

[6] B. Desrochers, S. Lacroix, and L. Jaulin, "Set-membership approach to the kidnapped robot problem," in *IEEE/RSJ IROS*, 2015, pp. 3715–3720.

[7] J. Ma, J. Zhao, J. Tian, A. L. Yuille, and Z. Tu, "Robust point matching via vector field consensus," *IEEE T. IP*, vol. 23, no. 4, pp. 1706–1721, 2014.

[8] J. Sivic and A. Zisserman, "Video google: A text retrieval approach to object matching in videos," in *IEEE ICCV*, 2003, pp. 1470–1477.

[9] K. Tanaka, "Cross-season place recognition using nbnn scene descriptor," in *IEEE/RSJ IROS*, 2015, pp. 729–735.

[10] ——, "Unsupervised part-based scene modeling for visual robot localization," in *IEEE ICRA*, 2015, pp. 6359–6365.

[11] R. Arandjelović and A. Zisserman, "Three things everyone should know to improve object retrieval," in *IEEE CVPR*, 2012, pp. 2911–2918.

[12] M. Milford and G. F. Wyeth, "Seqslam: Visual route-based navigation for sunny summer days and stormy winter nights," in *IEEE ICRA*, 2012, pp. 1643–1649.

[13] M. Ando, Y. Chokushi, K. Tanaka, and K. Yanagihara, "Leveraging image-based prior in cross-season place recognition," in *IEEE ICRA*, 2015.

[14] M. Douze, H. Jégou, H. Sandhawalia, L. Amsaleg, and C. Schmid, "Evaluation of gist descriptors for web-scale image search," in *Proc. ACM Int. Conf. Image and Video Retrieval*, 2009, pp. 19:1–19:8.

[15] N. Sünderhauf, P. Neubert, and P. Protzel, "Are we there yet? challenging seqslam on a 3000 km journey across all four seasons," *ICRA Workshop on Long-Term Autonomy held in conjunction*, 2013.

[16] M. Milford and G. Wyeth, "Persistent navigation and mapping using a biologically inspired slam system," *I. J. Robotic Res.*, vol. 29, no. 9, pp. 1131–1153, 2010.

[17] K. Ikeda and K. Tanaka, "Visual robot localization using compact binary landmarks," in *IEEE ICRA*, 2010, pp. 4397–4403.

[18] K. Min, L. Yang, J. Wright, L. Wu, X.-S. Hua, and Y. Ma, "Compact projection: Simple and efficient near neighbor search with practical memory requirements," in *IEEE CVPR*, 2010, pp. 3477–3484.

[19] A. Geiger, J. Ziegler, and C. Stiller, "Stereoscan: Dense 3d reconstruction in real-time," in *IEEE Intelligent Vehicles Symposium (IV)*, 2011, pp. 963–968.

[20] S. Thrun, W. Burgard, and D. Fox, *Probabilistic robotics*. MIT press, 2005.

[21] S. Se, D. Lowe, and J. Little, "Mobile robot localization and mapping with uncertainty using scale-invariant visual landmarks," *The international Journal of robotics Research*, vol. 21, no. 8, pp. 735–758, 2002.

[22] H. Lim, S. N. Sinha, M. F. Cohen, and M. Uyttendaele, "Real-time image-based 6-dof localization in large-scale environments," in *IEEE CVPR*, 2012, pp. 1043–1050.

[23] M. Cummins and P. M. Newman, "Appearance-only SLAM at large scale with fab-map 2.0," *I. J. Robotic Res.*, vol. 30, no. 9, pp. 1100–1123, 2011.

[24] M. Pandey and S. Lazebnik, "Scene recognition and weakly supervised object localization with deformable part-based models," in *IEEE ICCV*, 2011, pp. 1307–1314.

[25] B. Alexe, T. Deselaers, and V. Ferrari, "Measuring the objectness of image windows," *IEEE T. PAMI*, vol. 34, no. 11, pp. 2189–2202, 2012.

[26] T. Nagasaka and K. Tanaka, "An incremental scheme for dictionary-based compressive slam," in *IEEE/RSJ IROS*, 2011, pp. 872–879.

[27] H. Jégou, F. Perronnin, M. Douze, J. Sánchez, P. Pérez, and C. Schmid, "Aggregating local image descriptors into compact codes," *IEEE T. PAMI*, vol. 34, no. 9, pp. 1704–1716, 2012.

[28] K. Tanaka, Y. Chokushi, and M. Ando, "Mining visual phrases for long-term visual slam," in *IEEE/RSJ IROS*, 2014, pp. 136–142.